Dynamics of N_2 and N_2O Peaks During and After the Regeneration of Lean NO_x Trap

David Mráček [a], Petr Kočí [a,*] Miloš Marek [a], Jae-Soon Choi [b], Josh A. Pihl [b], William P. Partridge [b]

[a] *Institute of Chemical Technology, Prague, Department of Chemical Engineering, Technická 5, Prague 166 28, Czech Republic*

[b] *Fuels, Engines and Emissions Research Center, Oak Ridge National Laboratory, P.O. Box 2008, MS-6472, Oak Ridge, TN 37831, USA*

Abstract

The dynamics and selectivity of N_2 and N_2O formation during and after the regeneration of a commercial NO_x storage catalyst containing Pt, Pd, Rh, Ba on Ce/Zr, Mg/Al and Al oxides was studied with high-speed FTIR and SpaciMS analyzers. The lean/rich cycling experiments (60 s/5 s and 60 s/3 s) were performed in temperature range 200–400°C, using H_2, CO, and C_3H_6 individually for the reduction of adsorbed NO_x. Isotopically labeled ^{15}NO was employed in combination with Ar carrier gas in order to quantify N_2 product by mass spectrometry. N_2 and N_2O products were formed concurrently. The primary peaks appeared immediately after the rich-phase inception, and tailed off with the breakthrough of the reductant front (accompanied by NH_3 product). The secondary N_2 and N_2O peaks appeared at the rich-to-lean transition as a result of reactions between surface-deposited reductants/intermediates (CO, HC , NH_3, -NCO) and residual stored NO_x. At 200-300°C, up to 30% of N_2 and 50% of N_2O products originated from secondary peaks. The N_2O/N_2 selectivity ratio as well as the magnitude of secondary peaks decreased with temperature and duration of the rich phase. Among the three reductants, propene generated secondary N_2 peak up to the highest temperature. The primary N_2 peak exhibited a broadening shoulder aligned with the movement of reduction front from the zone where both NO_x and oxygen were stored to NO_x-free zone where only oxygen storage capacity was saturated. N_2 formed in the NO_x-free zone originated from the reaction of NH_3 with stored oxygen, while N_2O formation in this zone was very low.

Key words: NO_x storage catalyst, NO_x reduction, N_2O formation, N_2 formation, exhaust gas aftertreatment

Preprint submitted to Applied Catalysis B: Environmental *October 17, 2014*

1 Introduction

NO_x storage and reduction catalyst (NSRC), also known as Lean NO_x trap (LNT), is one of the technologies for aftertreatment of exhaust gas from lean gasoline and diesel engines in automotive applications. It enables NO_x adsorption under lean conditions when the amount of reducing species in the exhaust gas is not high enough to provide a sufficient NO_x reduction. Due to a limited NO_x storage capacity, the catalyst needs to be regenerated periodically by rich pulses containing excess of CO, H_2 and hydrocarbons from fuel.

The NO_x adsorption processes taking place under lean conditions are relatively slow. Over last two decades they have been studied extensively and are quite well understood [3,4,5,6,7]. On the other hand, the mechanisms of highly dynamic reduction of stored NO_x during the regeneration pulse are much less explored, particularly under few-seconds time scales relevant to real operation [12] when all processes are highly transient and catalyst is far from steady state conditions. The regeneration products include N_2 (desired final product), desorbed NO_x, NH_3 and N_2O.

When H_2 is used as the NO_x reducing agent, NH_3 is the main product of NO_x reduction in the fully reduced part of the catalyst. However, at the leading edge of the reduction front H_2 initially reacts with the surface-deposited NO_x over incompletely reduced PGM (platinum group metal) sites with a high local NO_x:H_2 ratio, and N_2O is likely to form under such conditions [20]. As the reduction front travels along the monolith channel, the primary N_2O peak is observed at the reactor outlet continuously before the breakthrough of the reduction front [17]. The NH_3 formed in the already reduced front part of the catalyst is transported by convection downstream into the still oxidized zone, where it reacts with the stored oxygen and NO_x to give N_2 and N_2O. This leads to a delayed breakthrough of ammonia at the reactor outlet [9,18,10,11,19]. After switch back to the lean conditions, a secondary N_2O peak can be observed at the reactor outlet at low-intermediate temperatures. This secondary peak comes from the reactions of the adsorbed reductants and reduction intermediates with the residual NO_x remaining on the surface after an incomplete regeneration [20]. During the regeneration with H_2 in the absence of CO and CO_2, the main reduction intermediate is adsorbed NH_3. The accumulation of NH_4NO_3 is not a major pathway for secondary N_2O formation at low temperatures because most stored NO_x are in the form of nitrites [8]. The secondary peak diminishes with a longer and more complete regeneration that does not leave enough residual NO_x and reduction intermediates on catalyst surface

* Corresponding author, tel: +420 22044 3293, fax: +420 22044 4320.
Email addresses: petr.koci@vscht.cz (Petr Kočí), partridgewp@ornl.gov (William P. Partridge).
URL: http://www.vscht.cz/monolith (Petr Kočí).

[20].

In case when CO is used as the reducing agent (or produced *in situ* from H_2 and CO_2 by reverse water gas shift), the mechanism of the stored NO_x reduction proceeds through an isocyanate (-NCO) surface intermediate [26,27,28,14] that can further react with NO, O_2, stored nitrites/nitrates and H_2O to form N_2O, N_2 or NH_3. Ammonia formed by hydrolysis of -NCO can further react with NO_x stored on the catalyst surface and thus further contribute to the overall NO_x conversion [29]. Despite the relatively fast rate of -NCO hydrolysis a substantial accumulation of isocyanates on catalyst surface was observed during rich phase also in presence of water and it was proposed that the decomposition of isocyanates can be responsible for the secondary N_2 and N_2O formation at the transition from rich to lean conditions [12,20,13]. The experimental study [31] demonstrated high selectivity of -NCO reaction with O_2 to molecular nitrogen, therefore the NO_x presence seems to be an important parameter driving the selectivity to N_2O [36]. However, in our recent publication [20] we have shown that the magnitude of the secondary N_2O peak does not depend on the presence of NO in the lean feed after the regeneration, and that the secondary N_2O peak (though smaller) can be formed even in the absence of oxygen. Therefore we proposed that the main source of the secondary N_2O peak is the reaction of residual stored NO_x with adsorbed reductants and reduction intermediates remaining on catalyst surface after the short rich phase.

In the case of reduction with hydrocarbons, a wider variety of organic species produced during rich conditions can contribute to the secondary N_2O formation upon the return to lean phase [30]. A parallel, indirect pathway of NO_x reduction by CO and hydrocarbons involves water gas shift and steam reforming reactions where hydrogen formed from CO and hydrocarbons in the presence of water acts as the NO_x reducing agent [16,33]. From the above-discussed observations it is obvious that the global NO_x reduction selectivity depends on many factors, e.g. temperature, spatiotemporal distribution of NO_x storage along the catalyst channel, reductant type, length of the rich period, and also on the actual state of platinum group metals (PGM) [15,16,17].

Even if tailpipe ammonia slip is generally undesired, NH_3 is a reactive by-product that can be utilized in further NO_x reduction, e.g. in the case of combined NO_x storage and NH_3-SCR catalytic systems [24,25]. In contrary, N_2O is an undesired by-product with low reactivity — although not toxic, it possesses a high global warming potential. Evolution of NO_x, NH_3 and N_2O can be readily measured with FTIR analyzers, however, the main N_2 product dynamics is more difficult to capture in full mixture and therefore it is usually not followed in detail.

In this paper we present the results of experimental study aiming to further

clarify the NO_x regeneration mechanisms over a fully formulated commercial NO_x storage catalyst under practical operating conditions with few seconds long rich phase. The catalyst contains platinum group metals (Pt, Pd, Rh) and Ba, CeZr, MgAl and Al oxides (lean-GDI, BMW 120i, Model Year 2009), which is a reference catalyst within the CLEERS research community [22]. Dynamics and selectivity of NO_x reduction towards all relevant N-products (N_2, N_2O and NH_3) were measured in dependence on temperature, reductant (H_2, CO, C_3H_6) and regeneration length relevant to practical application. To achieve that, a novel approach was developed that combines FTIR analysis with SpaciMS experiments using isotopically labeled ^{15}NO and Ar as carrier gas. Particular attention was given to N_2 and N_2O double-peak behavior first reported in [12] and further explored in recent studies [20,13]. These studies suggest that a significant part of the NO_x reduction products can be actually formed after the end of rich phase, which is enabled by the reactions of adsorbed reduction intermediates upon transition back to lean conditions. This effect has become a key part of the recently developed technology Di-Air [1,2] that uses high-frequency lean/rich cycling with very short rich pulses.

2 Experimental setup

The dynamics of products evolution was examined during lean/rich cycles in a bench flow reactor with synthetic exhaust gases. The lean and rich mixture composition is described in Table 1. The gas hourly space velocity (GHSV) was 30 000 h^{-1} and the tested temperature range was 200-400 °C. Two different regeneration lengths (3 or 5 s) were used while the lean phase length was kept constant (60 s).

Table 1
Inlet gas composition.

Component	Concentration	
	Lean	Rich
Nitrogen oxide (NO)	300 ppm	0 ppm
Oxygen (O_2)	10 %	0 %
Hydrogen (H_2)	0 %	3.4 %
Carbon monoxide (CO)	0 %	3.4 %
Propene (C_3H_6)	0 ppm	3780 ppm
Water (H_2O)	5 %	5 %
Carbon dioxide (CO_2)	0 %	0 %

The catalyst sample (2.1 cm in diameter, 3.8 cm long) was wrapped in Zetex

insulation tape and inserted into a horizontal quartz glass tube reactor, which was heated by an electric furnace. Inlet gas mixtures were prepared from pressurized gas cylinders (ultra high purity grade, Air Liquide) and pre-heated before entering the reactor. Precise amounts of desired gases were dosed through mass flow controllers (Unit Instruments Series 7300, Kinetics Electronics). Water was introduced by a high pressure liquid metering pump (Eldex) to a heated zone, vaporized instantly and added to the simulated exhaust mixture. A rapid switching 4-way valve was used to promptly alternate between the lean and rich gas mixtures [20,15].

First, temporally resolved evolution of products at the reactor outlet was analyzed by a high-speed FTIR gas analyzer (MKS 2030HS) in lean/rich cycling experiments using unlabeled NO and N_2 as carrier gas. The sampled gas was diluted after the reactor outlet to increase the flow-rate through the analyzer and to improve its dynamic response. The spatiotemporal profiles inside the catalyst channel were then obtained with the in-house developed spatially resolved capillary inlet mass spectrometer (SpaciMS) [23]. In order to enable accurate quantification of produced N_2 and N_2O in the SpaciMS experiments, standard ^{14}NO was replaced by isotopically labeled ^{15}NO and Ar was used as carrier gas. Gas was sampled from different axial locations inside a catalyst channel using a small capillary probe (200-μm outer diameter, 100-μm inner diameter) and fed (through an orifice) into a mass spectrometer for speciation. A relative longitudinal coordinate $0.00L$–$1.00L$ is used to denote location of the probe ($0.00L$ corresponds to the inlet, $1.00L$ corresponds to the outlet of the catalyst sample).

To further simplify the quantitative analysis of MS signals, CO_2 was excluded from the feed in all experiments (both FTIR and SpaciMS). Although CO_2 parent ion is identified at m/z 44, it contributes also to many other signals (e.g. m/z 16, 22, 28, 45, 46 [21]), particularly at high CO_2 levels around several percent. Even if certain amount of CO_2 was formed in the reactor in case of regeneration by CO and C_3H_6, this concentration was still an order of magnitude lower than that usually present in full exhaust mixture. We have shown in our recent paper [20] that CO_2 affects the catalyst performance in two ways: (i) decreases the NO_x storage capacity by competitive formation of carbonates on NO_x storage sites, and (ii) inhibits the regeneration with H_2 by reverse water gas shift reaction forming carbonyls on PGM sites and eventually gaseous CO. Despite these effects, we believe that the absence of CO_2 in our feed gas does not alter the conclusions we reach from this study. Considering the isotopically labeled ^{15}N, the species of interest were then measured by SpaciMS as follows: N_2 at m/z 30, N_2O at m/z 46, and NO at m/z 31.

3 Data processing

The processing of spatiotemporal data from SpaciMS experiments involved averaging of three lean/rich cycles obtained after a stationary cycling condition had been achieved to improve the signal/noise ratio and to minimize the errors in local maxima of narrow and sharp peaks where the measurement could become limited by sampling period. The following procedure was then used to convert the MS signals into concentrations.

Total amount of N_2O formed over the cycle was integrated from the FTIR measurements providing N_2O concentration at the reactor outlet. Correspondingly, the SpaciMS signal of m/z 46 (N_2O) at the sample outlet was also integrated. The ratio between those two integrals was then used as a scaling factor for the conversion of m/z 46 into N_2O concentration (constant factor applied to all spatial locations).

Total amount of N_2 product was then calculated from the N-atoms balance over the cycle, considering that the sum of formed N_2, N_2O, NH_3 and released NO_x during stationary lean/rich cycles has to be equal to the total amount of NO_x fed to the reactor. For a constant flowrate it is then:

$$2 \int_{t_1}^{t_2} y_{\mathrm{N_2}}^{\mathrm{out}} \, \mathrm{d}t = \int_{t_1}^{t_2} y_{\mathrm{NO_x}}^{\mathrm{in}} \, \mathrm{d}t - \int_{t_1}^{t_2} y_{\mathrm{NO_x}}^{\mathrm{out}} \, \mathrm{d}t - 2 \int_{t_1}^{t_2} y_{\mathrm{N_2O}}^{\mathrm{out}} \, \mathrm{d}t - \int_{t_1}^{t_2} y_{\mathrm{NH_3}}^{\mathrm{out}} \, \mathrm{d}t, \qquad (1)$$

where t_1 is the beginning of the lean phase and t_2 is the end of the rich phase (i.e., one complete lean/rich cycle). All integrals on the right hand side of Equation 1 were evaluated from FTIR measurements, enabling calculation of the integral N_2 product amount. The MS signal of m/z 30 (N_2) at the sample outlet was also integrated and the ratio between those two integrals was then used as a scaling factor for the conversion of m/z 30 signal into N_2 concentration (again, constant factor applied to all spatial locations).

A comparison of the FTIR and SpaciMS measurements (Figure 1) reveals that the FTIR signal is somewhat more dispersed than that measured by mass spectrometer. The broadening of peaks reflects a longer residence time of the sampled gas in the measurement cell of the FTIR (internal volume ca. 0.2 dm^3). Nevertheless, both signals exhibit similar dynamics as well as relative magnitude of primary and secondary peaks. This justifies the use of FTIR measured concentrations for scaling the SpaciMS data as well as compatibility of the experiments with isotopically labeled and unlabeled NO.

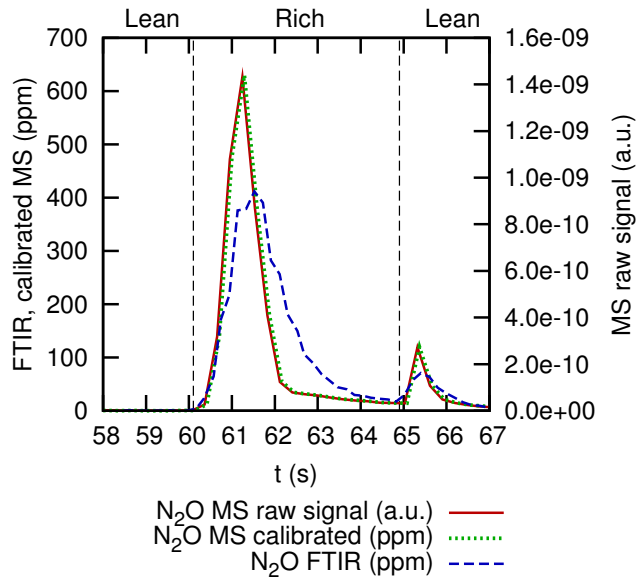

Figure 1. Comparison of the outlet N_2O signals from SpaciMS and FTIR analyzers during 5 s regeneration with C_3H_6 at 300 °C.

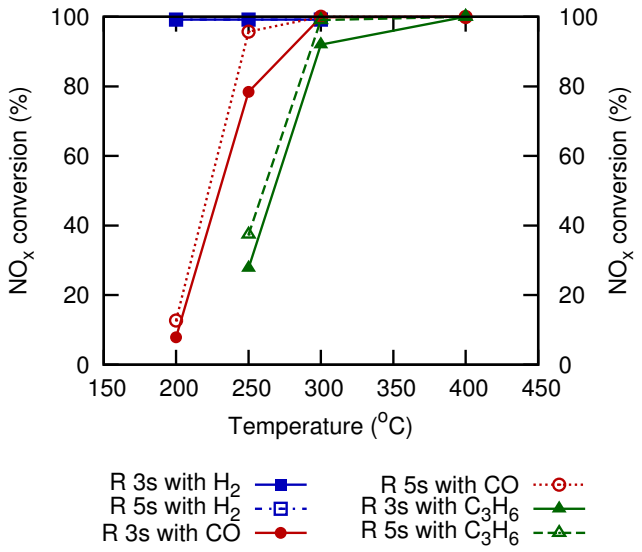

Figure 2. Integral NO_x conversions in lean/rich 60s/3s and 60s/5s cycles with different reductants.

4 Results and discussion

As it has been discussed in Introduction, the NO_x reduction dynamics, conversion and product selectivity during lean/rich cycles largely depends on the activity of reductant. The integral NO_x conversions achieved with H_2, CO and C_3H_6 are summarized in Figure 2. It can be seen that almost full conversion is achieved above the "light-off" temperature of each reductant. Pure hydro-

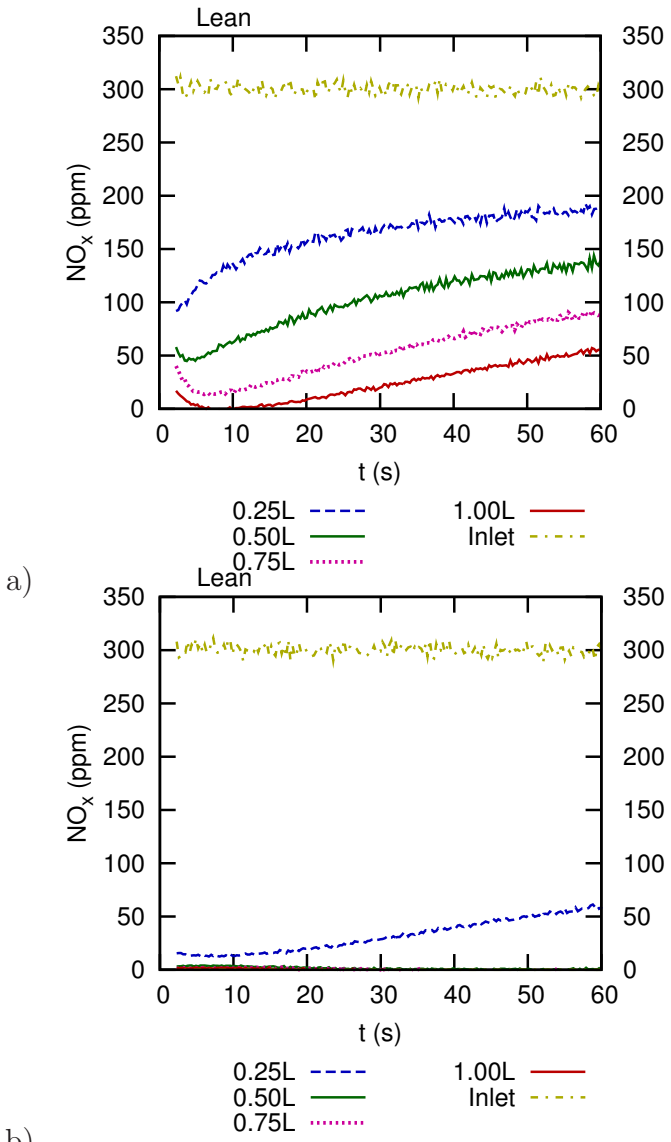

Figure 3. Spatiotemporal NO_x profiles during the lean phase of 60s/5s lean/rich cycles. a) Temperature 250 °C, C_3H_6 reductant (low NO_x conversion). b) Temperature 300 °C, CO reductant (high NO_x conversion).

gen is clearly the most active reductant providing full conversion already at 200°C. Somewhat lower efficiency of regeneration and a higher light-off temperature can be expected for real exhaust operation where CO_2 and CO are present, inhibiting the H_2 reactions [16,20]. The light-off temperature for CO-rich mixture is between 200-250 °C and temperature above 300 °C is needed for efficient LNT regeneration by C_3H_6. This comparison clearly illustrates that the effective NO_x storage capacity of the LNT sample over the studied range of temperatures is high enough to provide a complete adsorption of NO_x during 60 s long lean phase, and any loss of efficiency is caused just by incomplete regeneration during the applied rich phase.

Typical spatiotemporal profiles of NO_x in the gas flowing along the monolith

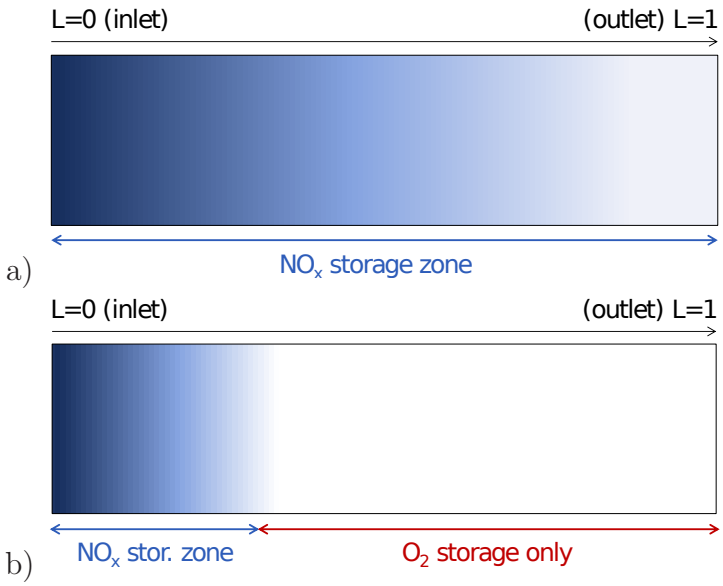

Figure 4. Schematics of stored NO_x profile along the catalyst length at the lean phase end. a) Low NO_x conversion, cycles with incomplete regeneration. b) High NO_x conversion, cycles with efficient regeneration.

channel during the lean/rich cycling are shown in Figure 3. The situation with an incomplete regeneration is shown in Figure 3a (C_3H_6 at 250 °C). Here the NO_x breakthrough at the catalyst outlet ($1.00L$) can be observed during the lean phase, because the adsorption efficiency is limited by a substantial amount of NO_x remaining on the surface from the previous cycles (consequence of incomplete regenerations). The corresponding spatial profile of the stored NO_x at the end of the lean phase is schematically depicted in Figure 4a. In contrast, when the regeneration is efficient (Figure 3b, CO at 300 °C), there is no lean NO_x breakthrough already at one half of the catalyst length ($0.50L$). It means that all NO_x is fully adsorbed within the first half of the catalyst ($0.00L$-$0.50L$), most of it in the first quarter ($0.00L$-$0.25L$). The corresponding spatial profile of the stored NO_x at the end of the lean phase is schematically depicted in Figure 4b.

The evolution of key component concentrations in the outlet gas during the 5 s regeneration with CO-rich mixture at 300°C can be seen in Figure 5. The time range shows the very end of lean phase (from 50 to 60 s), entire rich phase (from 60 to 65 s) and the very beginning of subsequent lean phase (from 65 s). There is no NO_x breakthrough at the end of the lean phase so that a high overall NO_x conversion is achieved at these operating conditions (cf. Figure 2). Immediately upon the switch to rich conditions, a minor NO_x slip peak appears as a residual of the rapidly released and unreduced NO_x. However, the major part of stored NO_x is reduced to N_2 (note the scale of two y-axes in Figure 5). The third peak that appears concurrently with NO_x and N_2 is N_2O. All these three primary peaks achieve their maxima shortly after the start of regeneration (around 61 s) and then start to decrease. The

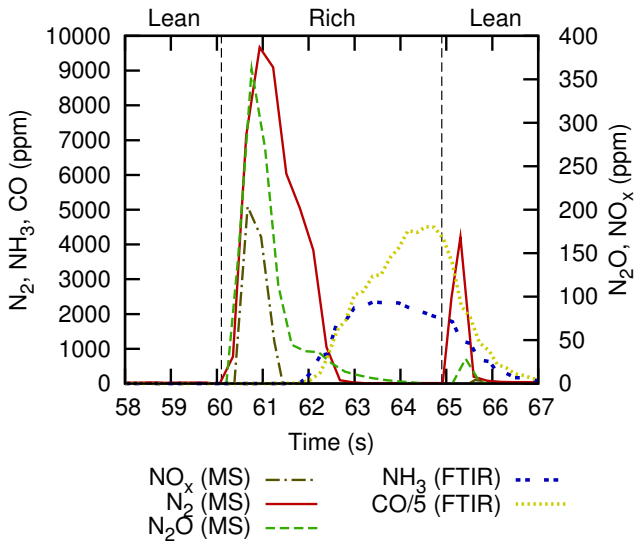

Figure 5. Outlet concentration dynamics of key components during the regeneration with CO-rich mixture at 300°C.

primary N_2 and N_2O peaks then exhibit an interesting feature — a broadening shoulder from ca. 61.5 s to 62.5 s. This will be discussed in more detail later.

Around two seconds after the start of regeneration, NH_3 appears at the catalyst outlet together with CO, indicating breakthrough of the reduction front — the PGM and fast OSC (oxygen storage capacity) sites along the entire catalyst have been reduced as well as large part of the previously stored NO_x. From this moment until the end of rich phase, the remaining part of NO_x on the catalyst surface is converted selectively to NH_3.

After the rich phase termination and switch back to lean conditions (time 65 s), NH_3 and CO concentrations fall down quickly.[1] At the same time, secondary N_2 and N_2O peaks appear at the reactor outlet as the products of reactions involving adsorbed reductants and reduction intermediates with residual stored NO_x under increasingly lean conditions. For CO-rich mixture at this temperature, the most relevant reduction intermediates are isocyanates [12,20,13]. It is known that isocyanates can be hydrolyzed to NH_3 (relevant mainly to rich conditions), oxidized readily by O_2 with a high selectivity to N_2 ([31]) or react with NO_x, the last reaction being the most probable source of N_2O by-product [20]. These reactions are completed within ca. 1-1.5 s so that from the time 66.5 s no more N-containing products are detected in the outlet gas and the catalyst returns fully to lean NO_x adsorption regime.

Spatiotemporal concentration profiles of N_2 and N_2O products (Figure 6) pro-

[1] The measured tails of NH_3 and CO peaks are extended by the signal dispersion in FTIR (measurement artifact, cf. the comparison of MS and FTIR signals in Figure 1).

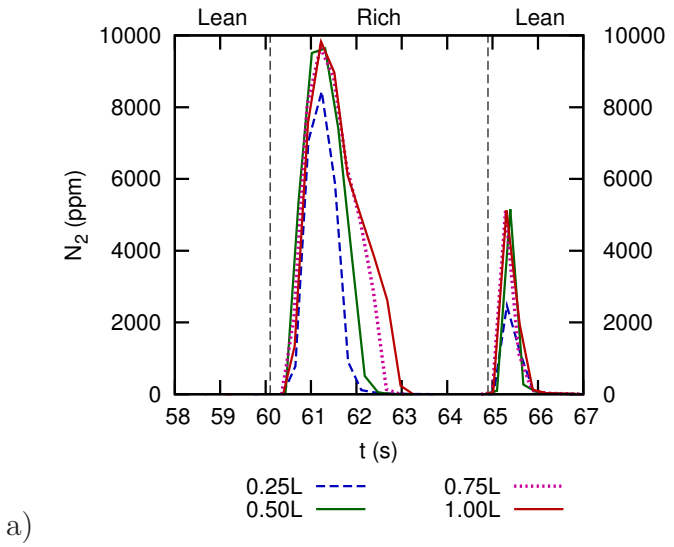

a)

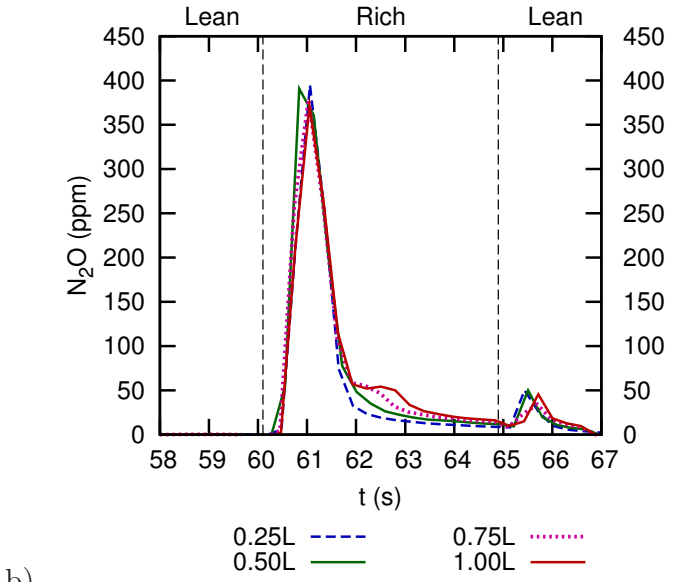

b)

Figure 6. Spatiotemporal concentration profiles of a) N_2 and b) N_2O products during LNT regeneration. 60s/5s lean/rich cycling with CO-rich mixture at 300°C (high NO_x conversion).

vide further details of the regeneration process. It can be seen that the main part of primary N_2 and N_2O peaks in the time interval 60.0–61.5 s is formed in the first quarter of the catalyst ($0.25L$) with no increase in the product concentrations at $0.50L$–$1.00L$. This is in line with the spatial distribution of stored NO_x prior to the rich phase (cf. Figure 4) and the fact that both N_2 and N_2O are formed during the reduction of stored NO_x at the rich regeneration front over incompletely reduced PGM sites (high O and NO coverage remaining from the lean phase) [17].

A progressively delayed and less intensive evolution of N_2 and N_2O products can be then observed at the locations $0.50L$–$1.00L$ during 61.5–63 s (Figure 6),

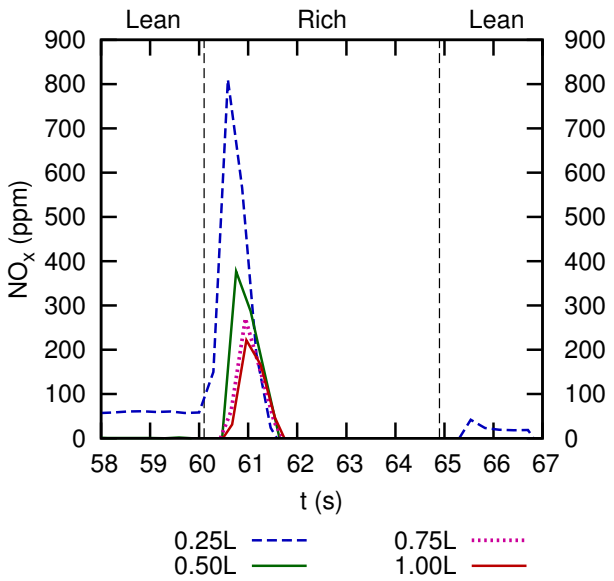

Figure 7. Spatiotemporal concentration profile of NO_x slip peak during LNT regeneration. 60s/5s lean/rich cycling with CO-rich mixture at 300°C (high NO_x conversion).

leading to a broadening shoulder of the primary peaks. Two main factors need to be considered when identifying the source of these delayed N_2 and N_2O products: First of all, the stored NO_x concentration is negligible in the zone $0.50L$–$1.00L$ (Figure 4). At the same time (61.5–63 s in Figure 6), no more N_2 and N_2O formation is detected in the first quarter of the catalyst where the NO_x are stored. The reason is that the sole local product of the NO_x reduction in that zone is already NH_3, as could be expected under fully established rich conditions on the catalyst surface. This is consistent with gradual NH_3 and CO breakthrough observed later at the catalyst outlet (Figure 5). Based collectively on these observations, we can conclude that the source of N_2 and N_2O products in the zone $0.50L$–$1.00L$ during 61.5–63.0 s (Figure 4) is the oxidation of NH_3 that has been formed upstream in the first quarter of the catalyst.

It was already demonstrated that the reaction of NH_3 with oxygen stored on Ce oxides (oxygen storage sites) is highly selective to N_2, while the reaction with stored NO_x significantly increases the selectivity to N_2O [15,20]. This is consistent with the relative magnitude of the product shoulder (61.5–63.0s) in Figure 5: The N_2 shoulder is two orders of magnitude higher than the N_2O shoulder.

It should be noted that even if all NO_x during the lean phase is trapped within the first quarter of the catalyst, the zone $0.50L$–$1.00L$ is not absolutely free from NO_x because the NO_x slip peak passed to the catalyst outlet at the beginning of the rich phase (cf. Figure 5) [15]. Partial re-adsorption of this NO_x

slip peak is evident from NO_x spatiotemporal concentration profiles shown in Figure 7. The re-adsorbed NO_x then contributed to minor N_2O formation from $0.50L$ to $1.00L$ during 61.5–63.0 s in Figure 5 as a by-product of NH_3+NO_x reaction.

After complete breakthrough of reduction front along the catalyst to the outlet (time 63.0 s in Figures 5 and 6), NH_3 is the sole product of NO_x reduction. Fully rich conditions are established at all locations — OSC is reduced, PGM sites are covered by excess of reductant species and substantial amount of isocyanate intermediates is accumulated on catalyst surface [20,13]. The reduction of NO_x stored on less accessible Ba sites farther from PGM as well as hydrolysis of isocyanates under these conditions is not completed within few seconds of rich regeneration.

Therefore, at the moment of switch back to lean conditions (time 65.0 s in Figures 5 and 6) the catalyst surface is generally covered by a residual amount of unreduced NO_x (relatively low in this case), adsorbed reductants (-CO) and reduction intermediates (-NCO). We can see in Figure 6 that the reactions of these species under increasingly lean conditions lead to formation of secondary N_2 and N_2O peaks mainly in the first quarter of the catalyst ($0.25L$). This spatial distribution is again in line with the fact that mostly the first quarter of the catalyst is used for NO_x storage under these cycling conditions (Figures 3b and 4b) so that the highest surface concentration of NO_x reduction intermediates is produced here during the rich phase.

Qualitatively similar spatiotemporal patterns were observed with all reductants in high conversion mode (above their light-off temperature, cf. Figure 2). A different type of product concentration profiles, typical for less active reductant and/or lower temperatures around the rich regeneration light-off, is shown in Figure 8 (reduction by C_3H_6 at 250°C). Before interpreting the results, let us remind that under these operating conditions the NO_x conversion is relatively low (Figure 2) and NO_x breaks through during the lean phase (Figure 3a) so that the NO_x storage zone covers entire catalyst length, even if most of NO_x are still stored in the front half of the catalyst (Figure 4a).

When the regeneration begins (time 60 s in Figure 8, N_2 and by-product N_2O are formed initially in the front quarter of the catalyst ($0.25L$) but with a small delay also at further locations ($0.50L$–$1.00L$) so that both N_2 and N_2O primary peaks grow along the entire catalyst length. Such a gradual build-up of products is in line with the profile of the stored NO_x prior to the regeneration. The progressive delay in product formation in downstream zones correlates with the movement of C_3H_6 reductant front towards the outlet, which is relatively fast under these conditions (low temperature, low effective oxygen storage capacity, slow reactions leading to incomplete C_3H_6 consumption).

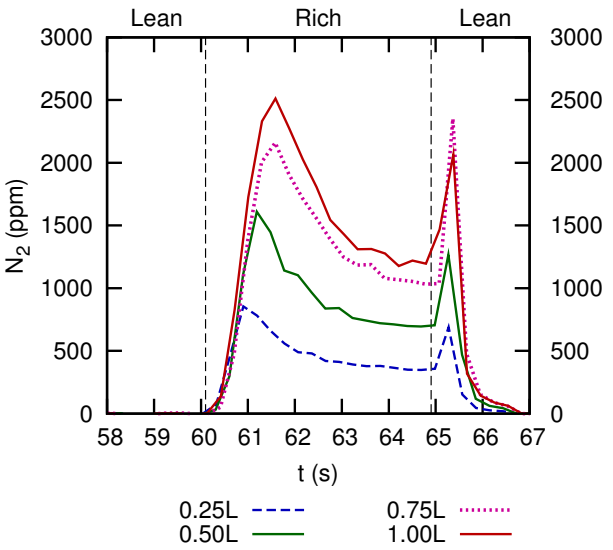

a)

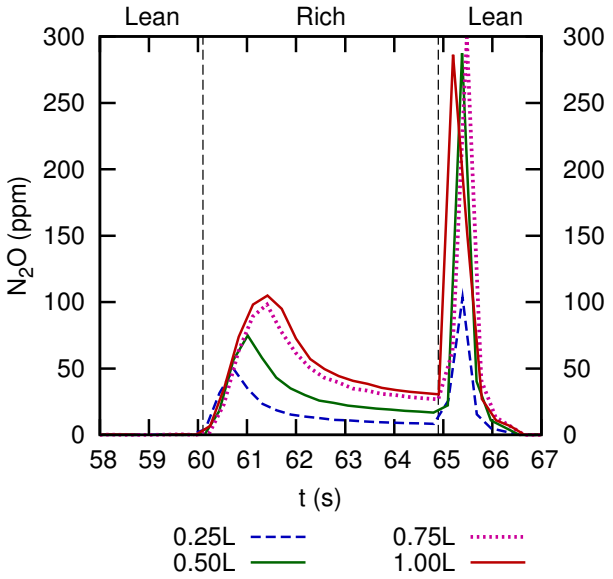

b)

Figure 8. Spatiotemporal concentration profiles of a) N_2 and b) N_2O products during LNT regeneration. 60s/5s lean/rich cycling with C_3H_6-rich mixture at 250°C (low NO_x conversion).

After the N_2 and N_2O primary peaks reach their maxima (time 61.5 s in Figure 8), the product formation rates decrease but still remain relatively high in comparison with the peak values. The N_2 and N_2O production continues along the entire catalyst length until the end of the rich phase. This indicates a kinetically controlled regeneration regime, i.e., the product formation is not locally limited by the presence of stored NO_x nor the availability of the reductant. The NO_x reduction rate correlates with the magnitude of primary N_2 peak (main product) and it is obviously much lower than with CO at 300°C (Figure 6). The NO_x reduction rate with C_3H_6 at 250°C is also much lower than the corresponding release rate of stored NO_x which leads to a significant

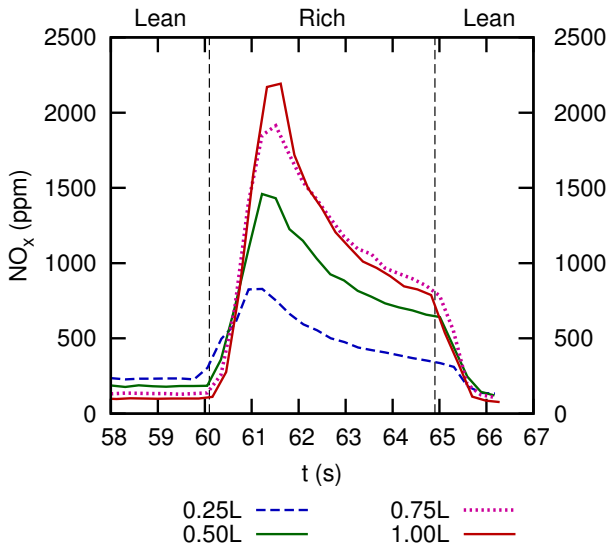

Figure 9. Spatiotemporal concentration profile of NO_x slip peak during LNT regeneration. Lean/rich cycling 60s/5s with C_3H_6-rich mixture at 250°C (low NO_x conversion).

rich-phase NO_x slip peak under these conditions (Figure 9).

Due to low NO_x reduction rate during the C_3H_6-rich regeneration at 250°C, the residual NO_x coverage at the end of rich phase is still quite high along the entire catalyst length. Furthermore, the catalyst surface is covered by adsorbed reductant (-C_3H_6) and reduction intermediates specific for hydrocarbons (not isocyanates). Even if there is no general agreement about the exact structure of these hydrocarbon-related intermediates [30,1], it can be concluded that their reactions after the switch back to lean conditions lead to the formation of secondary N_2 and N_2O peaks (time 65.0–67.0 s in Figure 8).

This behavior is qualitatively similar to CO-rich mixture (Figure 6) where isocyanates were key intermediates. Because in this case (Figure 8) the amount of residual unreduced NO_x is much higher and the lower temperature allows more reductant-related species to accumulate on the surface, the magnitude of secondary peak is comparable (N_2, Figure 8a) or even significantly higher (N_2O, Figure 8b) than that of primary one. This is further promoted by the fact that the reactions under rich conditions become self-inhibited by the reductant excess (PGM sites blocking), while under lean conditions the reactions accelerate because the PGM sites are freed from excessively high reductant coverage by reactions with oxygen [32]. However, this peak NO_x reduction rate is only transient and falls down again within one second (65.0–66.0 s in Figure 8) as all the adsorbed reductant/intermediate species are oxidized and there is no more driving force for NO_x reduction.

The relative contribution of secondary peaks to overall N_2 or N_2O product

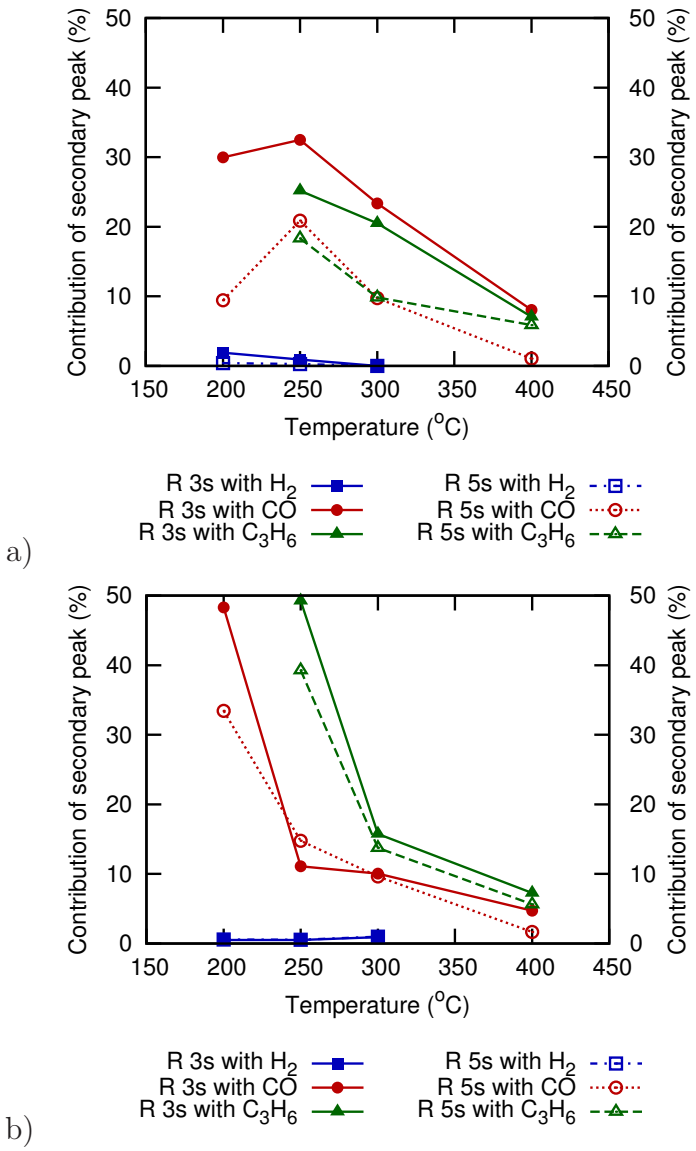

Figure 10. Relative contribution of secondary peak to overall yield of a product depending on operating conditions. a) N_2 product, b) N_2O product.

formed in dependence on the operating conditions is summarized in Figure 10. It can be seen that the importance of both N_2 and N_2O secondary peaks generally decrease with temperature, with N_2O exhibiting steeper dependence than N_2. For each reductant, the largest secondary peaks are generally observed at the regeneration light-off temperature (compare with NO_x conversions in Figure 2). At the light-off temperature, secondary peaks of N_2O represent up to 50 % of total N_2O emissions, while the contribution of secondary N_2 peaks to overall N_2 formation is around 30 % for the examined lean/rich timings. However, the contribution of secondary peaks to N_2O formation diminishes relatively fast with the increasing temperature, while secondary N_2 peaks decrease more slowly, indicating a change in the product selectivity.

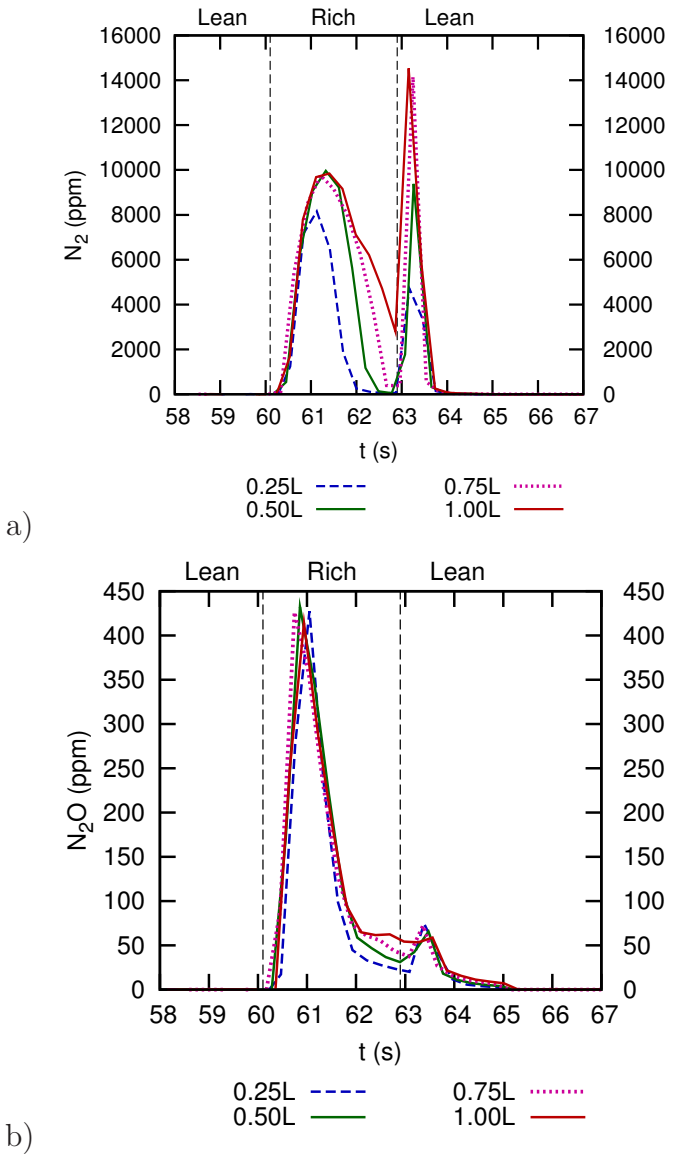

Figure 11. Spatiotemporal concentration profiles of a) N_2 and b) N_2O products during LNT regeneration. 60s/3s lean/rich cycling with CO-rich mixture at 300°C (high NO_x conversion, shorter regeneration).

The results in Figure 10 also show that relative contribution of both N_2O and N_2 secondary peaks increases with the decreasing rich phase length, which trend holds in the entire examined temperature range. The dependences on temperature and rich phase length are in line with the previously discussed mechanism of secondary peaks formation — lower temperature and shorter rich phase favor high coverages of both residual unreduced NO_x and adsorbed reductant intermediates. An example of the measured spatiotemporal concentration profiles for the shorter rich phase (3 s) is given in Figure 11. In comparison with the corresponding profiles at the same temperature and reductant but with a longer rich phase (Figure 7), it can be seen that the first

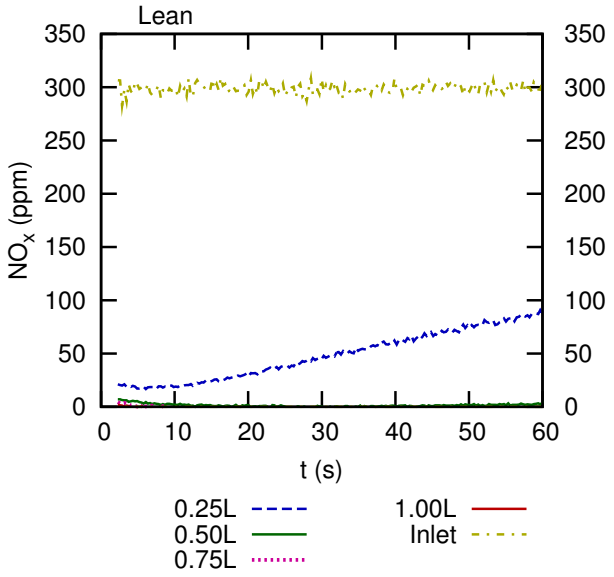

Figure 12. Spatiotemporal NO_x profiles during the lean phase of 60s/3s lean/rich cycles with CO-rich mixture at 300 °C (high NO_x conversion, shorter regeneration).

three seconds of regeneration (60–63 s) are similar. Only minor differences can be identified for 3 s rich phase in Figure 11: slightly slower movement of reduction front and thus more N_2 formed at $0.25L$–$0.50L$, and somewhat higher primary N_2O peak. These minor differences indicate a bit higher amount of NO_x stored on catalyst surface in the first half of catalyst length as a result of previous less complete regenerations. This is confirmed by the corresponding spatiotemporal NO_x concentration profile during the lean phase (Figure 12) showing a higher NO_x breakthrough at $0.25L$ than was observed in the case of 5 s regeneration (Figure 3b). Nevertheless, the NO_x capture is still complete at $0.50L$ so that a high NO_x conversion is maintained also with the shorter regeneration.

Indeed, the main difference between the dynamics of 3 s regeneration (Figure 11) and 5 s regeneration (Figure 6) relies in a higher magnitude of secondary peaks after the shorter regeneration. The magnitude of N_2 secondary peak appears to be more sensitive to rich phase length than that of N_2O. In the case of 3 s regeneration, the rich phase ended just at the beginning of NH_3 and CO breakthrough (compare with time 63 s in Figure 5) and the remaining surface NO_x and accumulated isocyanates were converted under increasingly lean conditions mostly to N_2 instead of NH_3 that would be the main product under continuing rich conditions.

The fraction of N_2O product in the sum of N_2 and N_2O (indicating the selectivity of NO_x reduction to products excluding NH_3) is shown in Figure 13. This fraction was calculated separately for primary and secondary peaks. At the rich regeneration light-off temperature (200°C for CO, 250°C for C_3H_6) the fraction of N_2O in secondary peak is significantly higher than in the pri-

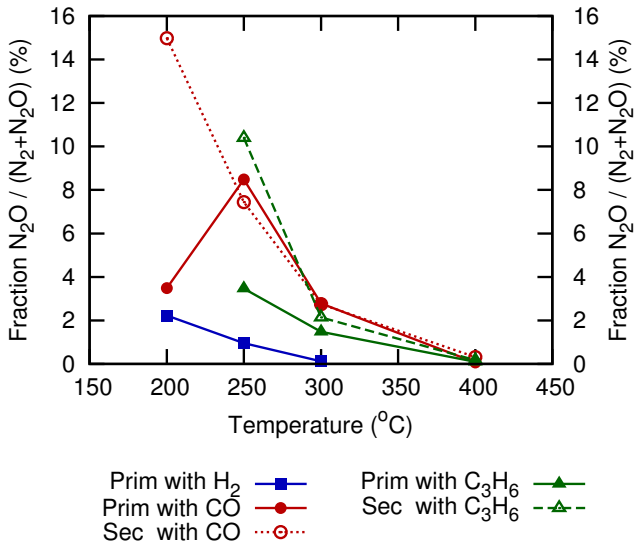

Figure 13. Fraction of N_2O product in the sum of N_2 and N_2O formed in primary and secondary peaks during lean/rich cycling 60s/5s.

mary peak, while at higher temperatures the N_2O fractions in both peaks are similar. The increased N_2O selectivity in secondary peaks around the light-off temperature is promoted by high residual coverage of stored NO_x as well as by gas-phase NO_x slip due to incomplete regeneration during rich phase — a high NO_x-to-reductant ratio generally favors N_2O formation. At higher temperatures, the NO_x reduction during rich phase is much more effective so both residual coverage of stored NO_x and gas-phase NO_x slip decrease. At 400 °C the N_2O formation in both primary and secondary peaks is further suppressed by increasing NO dissociation rate on PGM sites and fast interactions with reductants (preventing N_2O formation) as well as by an increasing rate of N_2O decomposition, so that the N_2O selectivity generally reaches negligible values for any reductant used.

5 Conclusions

The reported spatiotemporal concentration patterns of NO_x and NO_x reduction products during and after the LNT regeneration enabled to formulate general reaction mechanism leading to the formation of secondary N_2 and N_2O peaks. The results collectively suggest that the secondary peaks are formed by the reactions of adsorbed reductants and reduction intermediates with residual stored NO_x. Even if the exact nature of the adsorbed reduction intermediates may differ with temperature and the rich mixture composition (e.g., adsorbed NH_3 at lowest temperature during reduction with hydrogen, isocyanates during reduction with CO, and hydrocarbon-related intermediates with C_3H_6), this basic principle seems to hold over the entire range of operating condi-

tions. Lower temperatures and shorter rich phases favor high coverages of both residual stored NO_x and the reduction intermediates that together lead to formation of large secondary peaks upon the transient back to lean conditions.

During conventional lean/rich cycling using few seconds long rich phase, these secondary peaks are responsible for a significant part of N_2 and N_2O products formed at lower and intermediate temperatures (up to 30 and 50 %, respectively). With the increasing temperature the relative importance of secondary peaks decrease due to decreasing amount of adsorbed reductant intermediates as well as low residual coverage of stored NO_x, however, it is quite probable that with one order of magnitude shorter regeneration times and rapid lean/rich cycling strategy [1] the mechanisms for secondary peaks formation can still play an important role up to the highest temperatures.

Acknowledgements

This work has been financially supported by the Czech Ministry of Education (Project LH 12086) and the U.S. Department of Energy (DOE) Vehicle Technologies Office (program managers: Gurpreet Singh, Ken Howden and Leo Breton).

References

[1] Y Bisaiji, K Yoshida, M Inoue and K Umemoto, Development of Di-Air - A New Diesel deNOx System by Adsorbed Intermediate Reductants, SAE Int. J. Fuels Lubr. 5(1):380–388 (2012), doi:10.4271/2011-01-2089.

[2] C C Y Perng, V G Easterling and M P Harold, Fast lean-rich cycling for enhanced NO_x conversion on storage and reduction catalysts, Cat. Today **231** (2014), 125–134.

[3] W S Epling, L E Campbell, A Yezerets, N W Currier and J E Parks, Overview of the fundamental reactions and degradation mechanisms of NO_x storage/reduction catalysts, Cat. Rev. Sci. Eng. **46** (2004), 163–245.

[4] I Nova, L Castoldi, L Lietti, E Tronconi, P Forzatti, E Prinetto and G Ghiotti, NO_x adsorption study over Pt-Ba/alumina catalysts: FT-IR and pulse experiments, J. Cat. **222** (2004), 377–388.

[5] L Castoldi, I Nova, L Lietti and P Forzatti, Study of the effect of Ba loading for catalytic activity of Pt-Ba/Al_2O_3 model catalysts, Cat. Today **96** (2004), 43–52.

[6] E Fridell, M Skoglundh, B Westerberg, S Johansson and G Smedler, NO_x storage in barium-containing catalysts, J. Cat. **183** (1999), 196–209

[7] F Rodrigues, L Juste, C Potvin, J F Tempere, G Blanchard and G Djega-Mariadassou, NO_x storage on barium-containing three-way catalyst in the presence of CO_2, Cat. Lett. **72** (2001), 59–64

[8] J H Kwak, D H Mei, C W Yi, D H Kim, C H F Peden, L F Allard and J Szanyi, Understanding the natur of surface nitrates in BaO/gamma-γ-Al_2O_3 NO_x storage materials: A combined experimental and theoretical study, J. Cat. **261** (2009), 17–22

[9] L. Cumaranatunge, S.S. Mulla, A. Yezerets, N.W. Currier, W.N. Delgas, F.J. Ribeiro, Ammonia is a hydrogen carrier in the regeneration of $Pt/BaO/Al_2O_3$ NO_x traps with H_2, J. Catal. **246** (2007), 29–34

[10] R.D. Clayton, M.P. Harold, V. Balakotaiah, NO_x storage and reduction with H_2 on $Pt/BaO/\gamma$-Al_2O_3) monolith: Spatio-temporal resolution of product distribution, Appl. Catal. B-Environ. **84** (2008), 616–630.

[11] A. Lindholm, N.W. Currier, J. Li, A. Yezerets, L. Olsson, Detailed kinetic modeling of NO_x storage and reduction with hydrogen as the reducing agent and in the presence of CO_2 and H_2O over a Pt/Ba/Al catalyst, J. Catal. **258** (2008), 273–288.

[12] J P Breen, R Burch, C Fontaine-Gautrelet, C Hardacre and C Rioche, Insight into the key aspects of the regeneration process in the NO_x storage reduction (NSR) reaction probed using fast transient kinetics coupled with isotopically labelled (NO)-N-15 over Pt and Rh-containing Ba/γ-Al_2O_3 catalysts, Appl. Cat. B: Env. **81** (2008), 150–159.

[13] S Chansai, R Burch, C Hardacre and S Naito, Origin of double dinitrogen release feature during fast switching between lean and rich cycles for NO_x storage reduction catalysts, J. Cat. **317** (2014), 91–98.

[14] Y Ji, T J Toops and M Crocker, Isocyanate formation and reactivity on a Ba-based LNT catalyst studied by DRIFTS, Appl. Cat. B: Env. **140** (2013), 265–275.

[15] J-S Choi, W P Partridge, J A Pihl, M-Y Kim, P Kočí and C S Daw, Spatiotemporal distribution of NO_x storage and impact on NH_3 and N_2O selectivities during lean/rich cycling of a Ba-based lean NO_x trap catalyst, Cat. Today **184** (2012), 20–26.

[16] P Kočí, F Plát, J Štěpánek, Š Bártová, M Marek, M Kubíček, V Schmeisser, D Chatterjee and M Weibel, Global kinetic model for the regeneration of NO_x storage catalyst with CO, H_2 and C_3H_6 in the presence of CO_2 and H_2O, Cat. Today **147S** (2009), 257–264.

[17] P Kočí, Š Bártová, D Mráček, M Marek, J-S Choi, M-Y Kim, J A Pihl and W P Partridge, Effective Model for Prediction of N_2O Formation During the Regeneration of NO_x Storage Catalyst, Top. Cat. **56** (2013), 118–124.

[18] P Kočí, F Plát, J Štěpánek, M Kubíček and M Marek, Dynamics and selectivity of NO_x reduction in NO_x storage catalytic monolith, Cat. Today **137** (2008), 253–260.

[19] W P Partridge and J-S Choi, NH_3 formation and utilization in regeneration of $Pt/Ba/Al_2O_3$ NO_x storage-reduction catalyst with H_2, Appl. Cat. B: Env. **91** (2009), 144–151.

[20] Š Bártová, P Kočí, D Mráček, M Marek, J A Pihl, J-S Choi, T J Toops and W P Partridge, New Insights on N_2O Formation Pathways during Lean/Rich Cycling of a Commercial Lean NO_x Trap Catalyst, Cat. Today **231** (2014), 145–154.

[21] NIST web pages `http://webbook.nist.gov`, accessed 2014.

[22] CLEERS web pages `http://www.cleers.org`, accessed 2014.

[23] W P Partridge, J M E Storey, S A Lewis, R W Smithwick, G L DeVault, M J Cunningham, N W Currier and T M Yonushonis, Time-Resolved Measurements of Emission Transients By Mass Spectrometry, SAE Technical Paper 2000-01-2952 (2000).

[24] D Chatterjee, P Kočí, V Schmeißer, M Marek, M Weibel, B Krutzsch, Modelling of a combined NO_x storage and NH_3 -SCR catalytic system for Diesel exhaust gas aftertreatment, Cat. Today **151** (2010), 395–409.

[25] Y Liu, M P Harold and D Luss, Coupled NO_x storage and reduction and selective catalytic reduction using dual-layer monolithic catalysts, Appl. Cat. B: Env. **121** (2012), 239–251.

[26] I Nova, L Lietti, P Forzatti,F Frola, F Prinetto and G Ghiotti, Reaction Pathways in the Reduction of NO_x Species by CO over Pt-Ba/γ-Al_2O_3: Lean NO_x Trap Catalytic Systems, Top. Cat. **52** (2009), 1757–1761

[27] J-Y Luo and W S Epling, New insights into the promoting effect of H_2O on a model Pt/Ba/γ-Al_2O_3 NSR catalyst, Appl. Cat. B: Env. **97** (2010), 236–247.

[28] C D DiGiulio, V G Komvokis and M D Amiridis, *In situ* FTIR investigation of the role of surface isocyanates in the reduction of NO_x by CO and C_3H_6 over model Pt/BaO/γ-Al_2O_3 and Rh/BaO/γ-Al_2O_3 NO_x storage and reduction (NSR) catalysts, Cat. Today **184** (2012), 8–19.

[29] I Nova, L Lietti, P Forzatti, F Prinetto and G Ghiotti, Experimental investigation of the reduction of NO_x species by CO and H_2 over Pt-Ba/Al_2O_3 lean NO_x trap systems, Cat. Today **151** (2010), 330–337.

[30] E Joubert, X Courtois, P Marecot, C Canaff and D Duprez, The chemistry of $DeNO_x$ reactions over Pt/Al_2O_3: The oxime route to N_2 or N_2O, J. Cat. **243** (2006), 252–262.

[31] T Lesage, C Verrier, P Bazin, J Saussey and M Daturi, Studying the NO_x–trap mechanism over a Pt–Rh/Ba/Al_2O_3 catalyst by operando FT-IR spectroscopy, Phys. Chem. Chem. Phys. **5** (2003) 4435–4440.

[32] J-S Choi, W P Partridge and C S Daw, Spatially resolved in situ measurements of transient species breakthrough during cyclic, low-temperature regeneration of a monolithic Pt/K/Al_2O_3 NO_x storage-reduction catalyst, Appl. Catal. A **293** (2005) 24–40.

[33] P R Dasari, R Muncrief and M P Harold, Elucidating NH_3 formation during NO_x reduction by CO on Pt-BaO/Al_2O_3 in excess water, Cat. Today **184** (2012), 43–53.

[34] Y Ji, T J Toops, J A Pihl and M Crocker, NO_x storage and reduction in model lean NO_x trap catalysts studied by in situ DRIFTS, Appl. Cat. B: Env. **91** (2009), 329–338.

[35] L Lietti, P Forzatti, I Nova and E Tronconi, NO_x storage reduction over Pt-Ba/gamma-alu catalyst, J. Cat. **204** (2001), 175–191.

[36] L Castoldi, L Lietti, L Righini, P Forzatti, S Morandi and G Ghiotti, FTIR and Transient Reactivity Experiments of the Reduction by H_2, CO and HCs of NO Stored Over Pt-Ba/Al_2O_3 LNTs, Top. Cat. **56** (2013), 193–200.

*Graphical Abstract (for review)